

# Experimental Evidence of $\alpha$ -Olefin Readsorption in Fischer–Tropsch Synthesis on Ruthenium-Supported ETS-10 Titanium Silicate Catalysts

C. L. Bianchi and V. Ragaini

*Department of Physical Chemistry and Electrochemistry, University of Milan, Via Golgi, 19, 20133 Milan, Italy*

Received June 27, 1996; revised November 12, 1996; accepted December 9, 1996

Fischer–Tropsch synthesis seems to develop the following two consecutive paths: a primary process that involves the formation of  $\alpha$ -olefin products and a secondary process leading to the production of branched isomers and paraffins and requiring the readsorption of primary  $\alpha$ -olefin products. It was already shown by Iglesia *et al.* (E. Iglesia, S. C. Reyes, and R. J. Madon, *J. Catal.* **129**, 238 (1991)) that such readsorption steps are of fundamental importance for Ru catalysts and that they occur due to the slow diffusive removal of  $\alpha$ -olefins when the molecular size increases, this resulting in a long intraparticle residence time. In the present paper  $\alpha$ -olefins readsorption was enhanced by changing the metal distribution inside the pores of a titanium silicate (ETS-10), modified by ion exchange with alkali metal ions, used as a support for Ru-based catalysts.

© 1997 Academic Press

## 1. INTRODUCTION

Many studies have already shown that primary  $\alpha$ -olefin products undergo secondary reactions during Fischer–Tropsch synthesis (1–9). Especially Iglesia *et al.* (10–14) described the critical role played by the readsorption of  $\alpha$ -olefins and, to a much lesser extent, of internal olefins in hydrocarbon chain growth and demonstrated that these secondary reactions are crucial processes in Fischer–Tropsch synthesis. Herington (3) first suggested that surface chains terminate by desorption as paraffins and olefins and that olefins usually readsorb, initiate new growing chains and ultimately desorb again as larger hydrocarbons. These readsorption steps are repeated either until olefins are removed by diffusion and convection processes or until a surface chain terminates as unreactive paraffin (14).

In this paper ruthenium samples were prepared using as a support a special molecular sieve containing titanium in the framework position (ETS-10 by Engelhard (15)) and characterized by the total absence of acidic sites. It was reported (11) that the readsorption of  $\alpha$ -olefins is enhanced as their residence time and concentration within the catalyst pores increase. To achieve this, the intraparticle void (catalyst pores) was changed by modifying the ETS-10 commer-

cial form (mixed sodium–potassium form) by ion exchange with alkali metal ions and thus modifying the ruthenium distribution inside the support pores.

All the prepared samples were fully characterized and tested by Fischer–Tropsch synthesis.

## 2. EXPERIMENTAL

ETS-10 titanium silicate (commercial mixed sodium–potassium form,  $(\text{Na} + \text{K})/\text{Ti} = 1.8$ ;  $\text{Si}/\text{Ti} = 5.0$ ; pore radius  $r_p = 4 \times 10^{-10}$  m) was calcined at 773 K for 4 h. A suitable ion-exchange form of ETS-10 was prepared by multiple ion exchange with a  $\text{NH}_4\text{Cl}$  solution (1.0 N, Fluka) at 358 K for 20 h, according to the procedures proposed by Kuznicki (15) and then calcined at 673 K for 30 min to allow the decomposition of ammonia and to obtain the acidic form:



The acidic form then underwent further ion exchange with a  $M^I$  Cl solution (1.0 N, Fluka;  $M^I$  standing for Li, Na, K, Rb, or Cs) according to the above procedure.

Ruthenium catalysts (all 1 wt%) were prepared by slurry impregnation of the ion-exchanged  $M^I$ -ETS-10 samples with a solution of  $\text{Ru}(\text{NO})(\text{NO}_3)_3$  (Engelhard) in pure ethanol, and the ethanol excess was evaporated under vacuum.

All the samples were reduced, as suggested by Praliaud *et al.* (16), in flowing  $\text{H}_2$  ( $F_{\text{H}_2} = 80$  ml/min) at 623 K for 4 h and then characterized by means of XPS (M-Probe Instrument, SSI), ICP-AES (Jobin Yvon JY24), and TGA analyses. Ruthenium dispersion was measured by the single-introduction-back-sorption coupled method on the basis of irreversibly adsorbed hydrogen, as described elsewhere (17, 18).

Reaction tests were performed in a stainless-steel tubular reactor, coated with copper, designed especially for Fischer–Tropsch synthesis of hydrocarbons ( $C_n$ ;  $n < 15$ ) and described elsewhere (19). The reaction was carried out with a mixture of high purity CO and  $\text{H}_2$  (SIAD); the  $\text{H}_2/\text{CO}$  molar ratio of the inlet mixture was 2. The catalysts

(always 1 g of fresh sample for each run) were tested at 548 K, 500 kPa and a space velocity (SV) of  $9.0 \times 10^{-2}$  mmol CO/(mmolRu · s), also expressed as a GHSV of 2160 V/(V · h) (GHSV is defined as the hourly gas space velocity of the reactant flow at STP per total bed volume); the hydrocarbon products were analyzed on line by gas chromatography (19) and the C<sub>4</sub> fraction by means of GC-MSD (Hewlett Packard HP-5890 equipped with a mass selective detector HP-5971A, capillary column HP 1).

Since CO is the only detectable reactant, the mass balance calculation is based on carbon, presuming that the amount entering the reactor is equal to the amount leaving it. Therefore, the conversion is easily calculated by taking into account the total number of unreacted CO moles multiplied by the number of moles of carbon-containing species found at the exit.

### 3. RESULTS AND DISCUSSION

#### Characterization Results

A list of the prepared samples together with the data obtained by the XPS measurements is reported in Table 1. All the binding energy values were corrected taking Si2p at 103.0 eV as the internal reference. The ruthenium atoms are always present as RuO<sub>2</sub> species because of the reoxidation of the metal in contact with the atmosphere during sample mounting on the XPS sample holder. A reduction *in situ* of the samples with flowing hydrogen at 623 K for 4 h leads to the complete disappearance of the RuO<sub>2</sub> species, leaving only the metal Ru at  $279.9 \pm 0.2$  eV. No particular evidence was observed for the M<sup>f</sup> species which are present as M<sup>f+</sup> ions (before and after the reduction treatment).

Of particular interest is the Ru 3d<sub>5/2</sub>/Ti 2p<sub>3/2</sub> atomic ratio, which can be considered as a measure of the penetration of ruthenium inside the pores of the support. This ratio increases with increasing radius of the exchanged alkali metal so that, for instance, with an ion as large as Cs, the Ru/Ti ratio becomes very high, because the active metal can penetrate the pores only with great difficulty, due to the steric hindrance of the exchanged cation.

TABLE 1  
XPS Data<sup>a</sup> for Ru/M<sup>f</sup> Catalysts

Sample	Ti2p <sub>3/2</sub> (eV)	Ru3d <sub>5/2</sub> (eV)	M <sup>f</sup> (eV)	Ru/Ti	M <sup>f</sup> /Ti
ETS-10	459.7	—	—	—	—
Ru/H-ETS-10	459.3	280.9	—	0.11	—
Ru/Li-ETS-10	459.6	280.7	55.3 (1s)	0.12	0.9
Ru/Na-ETS-10	459.5	280.7	1072.5 (1s)	0.16	1.3
Ru/K-ETS-10	459.3	280.9	293.3 (1s)	0.26	0.8
Ru/Rb-ETS-10	459.5	280.8	110.8 (3d <sub>5/2</sub> )	0.34	1.4
Ru/Cs-ETS-10	459.7	280.6	724.9 (3d <sub>5/2</sub> )	0.80	1.5

<sup>a</sup> All the binding energy values are referred to Si2p.

TABLE 2  
Activity and Selectivity of the Samples

Sample	CO conversion (%)	CH <sub>4</sub> (%)	CO <sub>2</sub> (%)	C <sub>2+</sub> (%)	C <sub>3</sub> /C <sub>3-</sub> (SP/PP)	TOF (s <sup>-1</sup> × 10 <sup>2</sup> )	D <sub>M</sub>
Ru/Li-ETS-10	2.6	53.1	3.2	43.7	1.2	0.41	0.53
Ru/Li-ETS-10 <sup>a</sup>	13.4	45.4	5.4	49.2	1.5	0.71	0.53
Ru/Na-ETS-10	8.0	53.7	7.0	39.3	0.8	1.37	0.49
Ru/K-ETS-10	8.5	43.4	7.2	49.4	0.3	1.54	0.46
Ru/Rb-ETS-10	12.6	44.9	11.5	43.5	0.5	1.96	0.54
Ru/Cs-ETS-10	18.4	47.8	4.7	47.5	0.2	2.90	0.51

Note. T = 548 K; P = 500 kPa; GHSV = 2160 V/(V · h); H<sub>2</sub>/CO = 2; 1 g of fresh sample.

<sup>a</sup> Reaction performed under the same conditions, but with GHSV = 720 V/(V · h).

TGA measurements showed the total loss of ammonia during the thermal treatment and the stability of the sample up to 800 K; ICP-AES analysis confirmed  $1 \pm 0.02$  wt% ruthenium in all the samples.

H<sub>2</sub> chemisorption measurements provided metal dispersion (D<sub>M</sub>) which were similar for all samples (D<sub>M</sub> values are reported in Table 2).

#### Catalytic Test Results

Activity, selectivity, and TOF of all the samples tested by Fischer-Tropsch synthesis are reported in Table 2. TOFs were calculated by the equation  $\text{TOF} = F_{\text{CO}} \times C_{\text{CO}} / D_{\text{M}}$ , where F<sub>CO</sub> is the inlet CO flow, C<sub>CO</sub> is the CO molar conversion, and D<sub>M</sub> is the metal dispersion.

The Ru/Li-ETS-10 sample was tested under the same operating conditions, but at a different space velocity (GHSV = 720 V/(V · h)) in order to increase the CO conversion and to be able to compare the selectivity data of all the samples at similar conversion.

It is important to emphasize that for all the samples, the production of hydrocarbons is limited to C<sub>1</sub>-C<sub>7</sub> fractions. This is due to the reaction parameters and a significant "cage effect" of ETS-10 which acts as a molecular sieve, and thus prevents the classical Flory distribution of Fischer-Tropsch synthesis products (20).

A slight increase in the CO conversion was observed when the atomic radii of the exchanged cations were increased; a large production of C<sub>1</sub> species always occurred, caused both by the operation conditions (especially the H<sub>2</sub>/CO ratio) reported here and by the small size of the catalyst particles which influences the  $\chi$  parameter as defined in Ref. (14) [ $\chi = (R_0^2 \phi \theta_{\text{M}}) / r_{\text{p}}$ , where R<sub>0</sub> is the catalyst pellet radius,  $\phi$  is the pellet porosity,  $\theta_{\text{M}}$  is the density of surface metal atoms, and r<sub>p</sub> is the catalyst mean pore radius]. It was shown (14) that for low and high  $\chi$  values, obviously calculated by the authors for a different catalyst and

different operating conditions, the  $\text{CH}_4$  selectivity is very large and, in our case, a  $\chi = 47 \times 10^{16} \text{ m}^{-1}$  corresponds to a value found for the parameter in the high  $\text{CH}_4$  selectivity range.

The presence of different alkali metal ions in the samples play a role in the modification of the hydrocarbon selectivity. These alkali metal ions have different electronic effects on ruthenium, as shown by Everson and Mulder (21) and as suggested by Lang *et al.* (22) who hypothesized a direct interaction between  $M^{+}$  and the oxygen of CO. Moreover, Ertl *et al.* (23) argued that electropositive atoms, such as K, stabilize the molecular chemisorption and promote CO dissociation.

However, to explain the modification of selectivity, the change in residence time of the products inside the catalyst pores, as already reported by Iglesia *et al.* (10–13) must be considered. According to this hypothesis we can define a Primary Process (PP) as a process that makes  $\alpha$ -olefins and a Secondary Process (SP) during which the secondary reactions occur: the  $\alpha$ -olefins readsorb and consequently a higher production of  $\beta$ -olefins, branched paraffins and olefins, and linear paraffins takes place (Fig. 1)

In light of this interpretation, the paraffins to olefins ( $C_3/C_3^-$ ) ratio (Fig. 2) also represents an evaluation of SP in comparison to PP:

$$[\text{SP/PP}]_{C_3} \equiv C_3/C_3^-.$$

In the present case it is assumed that SP occurs much more frequently on Ru/Li-ETS-10 than on Ru/Cs-ETS-10. The Ru/Ti ratio, obtained by XPS, may offer an explanation. This ratio, as mentioned above, can be considered as a measure of the penetration of the ruthenium atoms inside the pores of the support; SP is enhanced when the primary products have the possibility of readsorbing during their back-diffusion from the catalyst pores and, therefore, when the active metal is present even if it is within the pores. A comparison of possible pore structures in Ru/Li-ETS-10 and Ru/Cs-ETS-10 is shown in Fig. 3: the intraparticle void is probably modified, thus changing the kind of cation in the framework structure, as already reported in (24). The

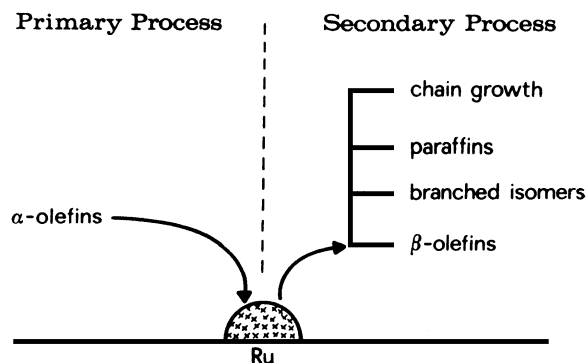


FIG. 1. Schematic diagram of primary and secondary process.

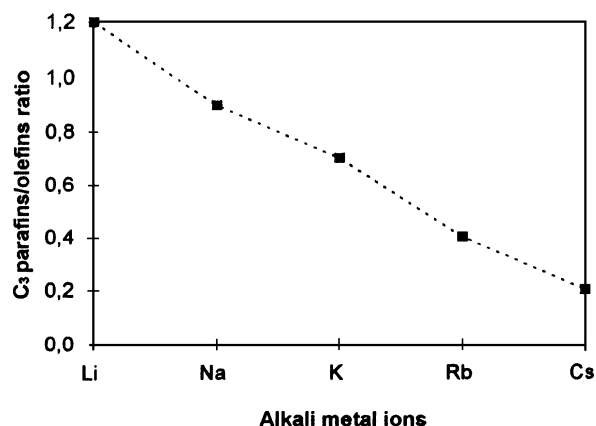


FIG. 2.  $C_3$  paraffins/olefins ratio for Ru 1% on M-ETS-10 (M stands for alkali metal ions).

more the Ru/Ti ratio decreases, the more the SP/PP ratio increases, because  $\alpha$ -olefins residence time increases.

Taking into account the  $C_4$  hydrocarbon production, this fraction was analyzed in detail by GC/MSD in order to identify precisely all the peaks revealed by on-line GC analysis.

Figure 4 shows two different chromatograms for Ru/Na-ETS-10 (Fig. 4a) and Ru/Cs-ETS-10 (Fig. 4b). From the GC/MSD analysis it was possible to assign the corresponding compound to each GC peak: A for isobutene, B for isobutane, C for 1-butene ( $\alpha$ -olefin), D for butane, E and E' for 2-butene (*cis* and *trans* form, respectively).

Figure 4 is interesting because it shows that some of the catalysts have different product distribution: generally speaking, isoolefins (peak A) and  $\beta$ -olefins (peaks E and E') are not always present, while isoparaffins (peak B) and  $\alpha$ -olefin (peak C) are always detected.

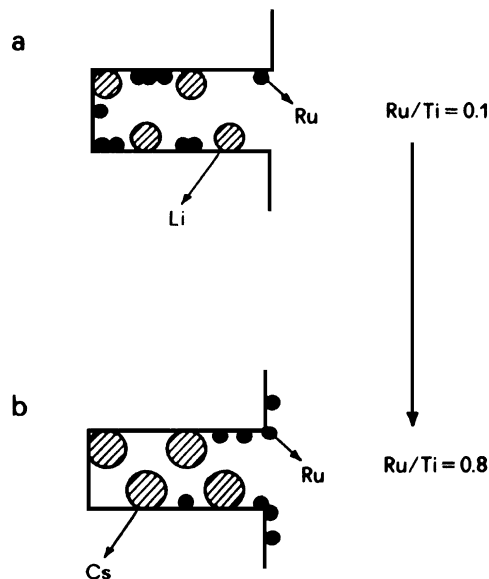


FIG. 3. Pore structure in the presence of Li or Cs atoms.

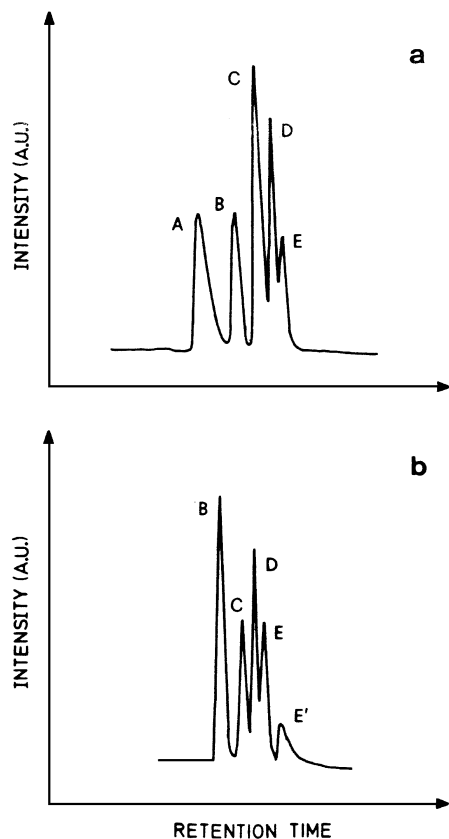


FIG. 4. GC peak of the  $C_4$  hydrocarbon fraction: A, isobutene; B, isobutane; C, 1-butene ( $\alpha$ -olefin); D, butane; E and E', 2-butene (*cis* and *trans* forms, respectively).

Based on these results a more precise SP/PP ratio was calculated:

$$[\text{SP/PP}]_{C_4} \equiv (\text{A} + \text{B} + \text{D} + \text{E} + \text{E}')/\text{C}.$$

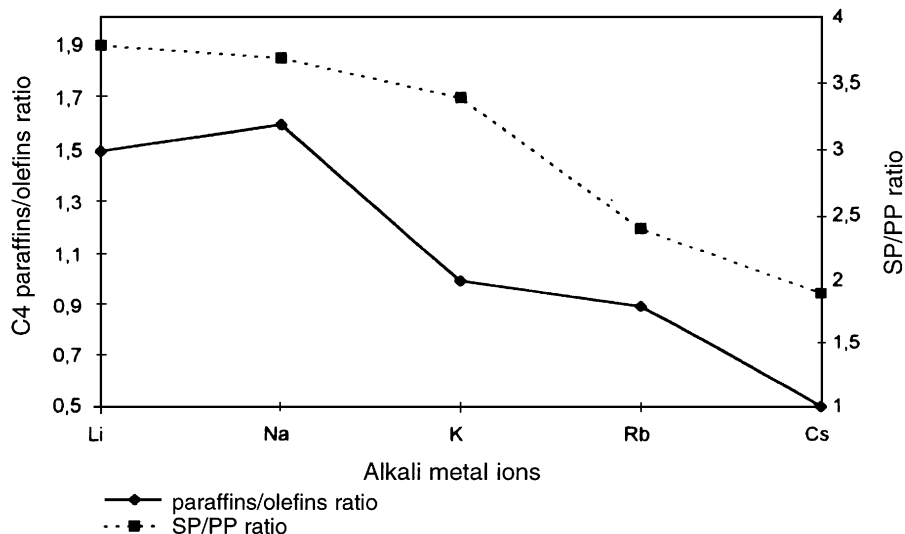


FIG. 5.  $C_4$  paraffins/olefins ratio and SP/PP ratio for Ru 1% on  $M$ -ETS-10 ( $M$  stands for alkali metal ions). Data shown in Table 3.

TABLE 3

Production of Hydrocarbons in the  $C_4$  Fraction

Sample	SP/PP	$\alpha$ -Olefin (%) (PP)	$\beta$ -Olefin (%) (SP)	Isocompound (%) (SP)	Paraffins (%) (SP)
Ru/Li-ETS-10	3.8	20	18	40	19
Ru/Li-ETS-10 <sup>a</sup>	4.0	20	21	39	20
Ru/Na-ETS-10	3.7	19	7	52	11
Ru/K-ETS-10	3.4	23	25	33	19
Ru/Rb-ETS-10	2.4	29	24	20	27
Ru/Cs-ETS-10	1.9	33	30	4	33

<sup>a</sup> Reaction performed under the same conditions, but with GHSV = 720 V/(V · h).

Table 3 lists all the data for the  $C_4$  fraction.

The experimental results (see also Fig. 5) highlighted a net decrease both in the paraffins/olefins ratio and in the SP/PP ratio, as already observed for the  $C_3$  fraction.

Finally, there are very different TOF values for CO hydrogenation (reported in Table 2). This fact suggests that the increase in the activity may be caused by electronic effects due to the different textural alkali metals and/or by the different distribution of noble metals in the support pores, while the dispersion was practically constant on all the samples. In fact, the presence of active metal at different depths in the pores may severely limit CO transport and thus cause a generally low TOF, as reported by Iglesia *et al.* (see Ref. 14, Table VII, p. 289) who compared two totally different cobalt catalysts: an-egg-shell pellet (comparable to Ru/Cs-ETS-10 sample) and an even large pellet (comparable to Ru/Li-ETS-10 sample). The egg-shell catalyst showed a higher TOF value than the penetrated one.

#### 4. CONCLUSIONS

The experimental results presented in this work confirm that  $\alpha$ -olefin readsorption is an important aspect of Fischer-Tropsch synthesis and that this phenomenon can be enhanced by modifying the pore structure of the support. In the present case, a molecular sieve containing titanium in the framework position and characterized by the absence of acidic sites was exchanged with different alkali metal ions in order to modify the intraparticle void. Therefore, the active metal, introduced by impregnation, was distributed on the support surface in different ways: when the atomic radius is low, as for the lithium ion, ruthenium can penetrate the deep part of the pore, while the noble metal must remain at the pore entrance when the atomic radius is large, as for the cesium ion. These two extremes result in two different reaction path ways: in the first case, the primary products ( $\alpha$ -olefins) can readsorb during their diffusion out of the pore, thus leading to an increase in the number of secondary products; in the latter case, however,  $\alpha$ -olefins do not have as many sites on which to readsorb, and the main products come from PP.

#### ACKNOWLEDGMENT

The authors thank Dr. C. Cavenaghi (Engelhard, Italy) for fruitful discussions.

#### REFERENCES

1. Smith, D. R., Hawk, C. O., and Golden, P. L., *J. Am. Chem. Soc.* **52**, 3221 (1930).
2. Craxford, S. R., *Trans. Faraday Soc.* **64**, 447 (1939).
3. Herington, E. F. G., *Chem. Ind.* **65**, 346 (1946).
4. Pichler, H., Schulz, H., and Elstner, M., *Brennst.-Chem.* **48**, 78 (1967).
5. Koelbel, H., and Ruschenburg, E., *Brennst.-Chem.* **35**, 161 (1954).
6. Golovina, O. A., Sakharov, M. M., Roginskii, S. Z., and Dokukina, E. S., *Russ. J. Phys. Chem.* **33**, 471 (1959).
7. Roginskii, S. Z., "Proceedings, 3rd International Congress on Catalysis, Amsterdam, 1964," p. 939. Wiley, New York, 1965.
8. Hall, W. K., Kokes, R. J., and Emmett, P. H., *J. Am. Chem. Soc.* **82**, 1027 (1960).
9. Novak, S., Madon, R. J., and Suhl, H., *J. Catal.* **77**, 141 (1982).
10. Iglesia, E., Reyes, S. C., and Madon, R. J., *J. Catal.* **129**, 238 (1991).
11. Madon, R. J., Reyes, S. C., and Iglesia, E., *J. Phys. Chem.* **95**, 7795 (1991).
12. Iglesia, E., Reyes, S. C., Madon, R. J., and Soled, S. L., in "Advances in Catalysis and Related Subjects" (H. Pines, D. D. Eley, and P. B. Weisz, Eds.), Vol. 38. Academic Press, New York, 1992.
13. Madon, R. J., and Iglesia, E., *J. Catal.* **139**, 576 (1993).
14. Iglesia, E., Reyes, S. C., Madon, R. J. and Soled, S. L., in "Advances in Catalysis and Related Subjects," (H. Pines, D. D. Eley, and P. B. Weisz, Eds.), Vol. 39. Academic Press, New York, 1993.
15. (a) Kuznicki, S. M., U.S. Patent 4,853,202 (1989); (b) Kuznicki, S. M., U.S. Patent 4,938,939 (1990).
16. Praliaud, H., Dalmon, J. S., Miradatos, C., and Martin, G. S., *J. Catal.* **97**, 344 (1986).
17. Giannantonio, R., Ragaini, V., and Magni, P., *J. Catal.* **146**, 103 (1994).
18. Ragaini, V., Giannantonio, R., Magni, P., Lucarelli, L., and Leofanti, G., *J. Catal.* **146**, 123 (1994).
19. Ragaini, V., Carli, R., Bianchi, C. L., Lorenzetti, D., and Vergani, G., *Appl. Catal.* **139**, 17 (1996).
20. (a) Friedl, R. A., and Anderson, R. B., *J. Am. Chem. Soc.* **72**, 1212 (1950); (b) Anderson, R. B., *J. Catal.* **55**, 114 (1978).
21. Everson, R. C., and Mulder, H., *J. Catal.* **143**, 166 (1993).
22. Lang, N. D., Holloway, S., and Nørskov, J. K., *Surf. Sci.* **150**, 24 (1985).
23. Ertl, G. Lee, S. B., and Weiss, M., *Surf. Sci.* **111**, L711 (1981).
24. Carli, R., Bianchi, C. L., and Ragaini, V., *Catal. Lett.* **33**, 49 (1995).